

CONTACT INTERACTION OF AN UNDERGROUND PIPELINE WITH SOIL UNDER DYNAMIC IMPACTS

Karim Sultanov

Institute of Mechanics and Seismic Stability of Structures named after
M.T. Urazbaev Uzbekistan Academy of Sciences, Tashkent, Uzbekistan

ORCID iD: Karim Sultanov

<https://orcid.org/0000-0002-5526-9862>

Abstract. *The interaction between a semi-infinite underground pipeline and the surrounding soil during longitudinal seismic wave propagation is examined in the article. The wave travels through the soil with its front perpendicular to the pipeline's axis, and the nonlinear laws of interaction (friction) on the surface of their contact, including the Amonton-Coulomb law, are used to solve related wave problems for the pipeline and soil. The method of characteristics and the finite difference method are sequentially used to solve these problems numerically. The implementation of the law of interaction (friction) processes is shown, depending on the parameters of the wave in soil and the mechanical characteristics of soil. It was determined that a wave in soil that involves the pipeline generates a powerful wave in the pipeline. The amplitude of this wave is many times greater than the amplitude of the wave in soil, and it propagates through the pipeline without attenuation. The dependences of the amplitude of this wave on the parameters of the law of friction, waves in soil, and the mechanical characteristics of soil are determined.*

Key words: *Pipeline, Soil, Underground, Law of interaction, Friction, Wave, Numerical solution*

1. INTRODUCTION

As noted by Popov and Heß [1], contact and friction are significant phenomena in various fields of science and technology, including underground utilities. Underground pipelines serve as essential engineering life support lines for the population and industry, making them crucial for the economy of any country. Hence, ensuring the strength and durability of underground pipelines is a critical and relevant problem. When an underground pipeline is subjected to external dynamic impacts, primarily seismic, it interacts with the surrounding soil, resulting in a frictional force on the surface of their contact. The complexity of these friction forces is evident from experimental results obtained by Sultanov [2].

Received: December 27, 2023 / Accepted March 28, 2024

Corresponding author: Karim Sultanov

Institute of Mechanics and Seismic Stability of Structures named after M.T. Urazbaev, Academy of Sciences of the Republic of Uzbekistan, Durmon yuli street 33, 100125 Tashkent, Uzbekistan

E-mail: sultanov.karim@mail.ru

The specific characteristics of the contact and friction between underground pipelines and soil are notable due to the significant difference in strength between a steel pipeline and loamy soil. This specificity manifests in the fact that the strength of contact between soil particles and the outer surface of the pipeline is greater than the contact between the particles of soil [2]. This phenomenon occurs because, over time, soil particles stick to the pipeline due to cohesion processes and the corrosion properties of the steel pipeline, as noted by Sultanov [2].

When an underground pipeline moves or shifts relatively to the soil, it involves the soil particles in a specific thickness called the contact layer [2, 3]. This interaction between the pipeline and soil results in a complex friction process. The law of interaction between the underground pipeline and soil is quite complex and has been developed based on the results of fundamental experimental research obtained by Sultanov [2] and Sultanov and Vatin [3].

The interaction of an underground pipeline with the surrounding soil, under the impact of dynamic (seismic) loads, considering the free (daytime) earth surface is a complex three-dimensional spatial wave problem. This problem can be solved using numerical modeling methods. However, great difficulties arise when implementing numerical modeling in a three-dimensional solution domain. This problem, with reasonable simplifications, is reduced to two one-dimensional wave problems [3].

Thus, when seismic waves propagate in the “pipeline-soil” system, we accept a nonlinear law on the surface of their contact, which includes the Amonton-Coulomb law [2]. It is known that when solid bodies interact by the Amonton-Coulomb law, the friction force instantly reaches its limiting value, that is, the rate of change of the friction force is equal to infinity. At the beginning of the interaction curve, there is a small-width section where the friction force increases to a limiting value, depending on the relative displacement. When the pipeline interacts with soil, which is an essentially “soft” body, this pre-limit section significantly expands and becomes complex and curvilinear, as noted by Sultanov [2] and Sultanov and Vatin [3].

In the limiting section, the Amonton-Coulomb law is satisfied. In the pipeline-soil system, during the propagation of high-frequency seismic waves in soil with a frequency $f=50\text{ s}^{-1}$ and an amplitude of 0.5 MPa, by the interaction law, 50 and more times increase in the amplitude of longitudinal stresses was observed in the pipeline compared to the stress amplitude in soil [3]. Here, the problem is considered for the case of propagation of a low-frequency seismic wave in soil and changes in longitudinal stresses in the pipeline.

Underground pipelines, as life support lines for the population and industry, are currently of significant importance in the global economy. As the means of conveying liquid and gaseous products, water, etc., underground pipelines are the most profitable and economical structures. However, the destruction of operating underground pipelines under external influences can lead to huge environmental and economic disasters. One of these external influences is seismic loads. An analysis conducted by Kwong et al. [4] clearly show the aftermath of strong earthquakes. One of the main issues considered by Musa [5] is the condition of the contact of various structures with media. In the problem of interaction of an underground pipeline with the surrounding soil, the main issue is the proper selection of interaction law, adequate to the interaction process. The stress-strain state of the pipeline was determined, and, based on this, its seismic resistance was assessed by Fan et al. [6] and Popov [7].

Zhang et al. [8], Xue et al. [9], Yiğit et al. [10], and Demirci et al. [11] considered the mechanical behavior of underground pipelines crossing a fault. Numerous authors [12-17] discussed issues of interaction between an underground pipeline and soil. Dai et al. [18] and Huang et al. [19] showed how important it is to correctly model the underground pipeline

interaction with soil under the impact of a seismic wave. It was proven that Goodman's model, consisting of spring deformation and frictional contact, agrees with reality. Sarvanis et al. [20] developed a model of the longitudinal interaction of an underground pipeline with soil, considering the dilatancy of the contact layer of soil. Soil dilatancy determines the increase in soil pressure on the pipeline. Sarvanis et al. [20], based on in-depth experimental and theoretical studies, determined that soil strain could cause significant stresses in the pipeline body, leading to rupture. Psyrras et al. [21] and Bakhodirov et al. [22] made an in-depth analysis of extensive literature sources to show that correct modeling of the interaction process of an underground pipeline with soil is important in the reliable determination of stresses in the pipe. Issues of modeling the viscoelastic properties of materials, including soils, numerical modeling of dynamic processes, and the behavior of underground pipelines under seismic impacts were examined in references [23- 27].

The study aims to determine the longitudinal stresses in underground main pipelines under the impact of low-frequency seismic waves, based on the nonlinear laws of interaction (friction) of an underground pipeline with soil.

2. LAW OF LONGITUDINAL INTERACTION OF AN UNDERGROUND PIPELINE WITH SOIL

Summarizing the results obtained by Sultanov [2] and Sultanov and Vatin [3], a schematic representation of the pipeline-soil interaction is shown in Fig.1, where τ is the shear stress arising in the process of the pipeline interaction with soil, $u = u_g - u_c$ is the relative displacement, u_g is the absolute longitudinal displacement of soil in the pipeline's axis direction, and u_c is the absolute longitudinal displacement of the pipeline.

The research conducted by Sultanov [2], Sultanov and Vatin [3], and Bakhodirov et al. [22] show that shear stress τ appears in a certain contact layer of soil surrounding the pipeline. Relative displacement does not occur since due to cohesion processes, directly on the pipe-soil contact surface, soil particles strongly cohere to the outer surface of the pipe. Relative displacement occurs in the thickness of the contact layer Δ [2].

Curve 1 ($OACE$) in Fig. 1 corresponds to the process of the complete first cycle of interaction when the soil contact layer is not damaged. This is the first cycle of the interaction of an embedded (for a long time) pipeline. If this cycle passes completely along the OAC curve, then at point C , the contact layer is damaged and the pipeline interacts with the destroyed soil layer along the CE line. Subsequent cycles of interaction between the underground pipeline and soil follow the dashed curve 2 (OC).

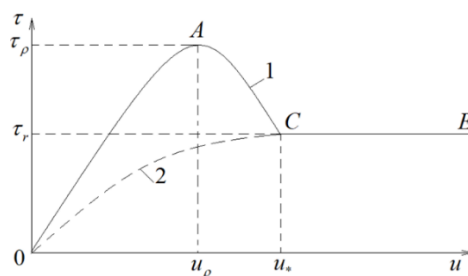


Fig. 1 Diagrams of the interaction of an underground pipeline with soil. 1 - for undamaged contact layer of soil, 2 - for damaged contact layer of soil

In the first case, the peak value of the shear stress $\tau=\tau_p$ appears at the value of the relative displacement $u=u_p$. It can be assumed that in the first cycle, up to 70% of the relative displacement u_p , the interaction occurs elastically, i.e. elastic bonds between particles in the contact layer of soil are kept. The law of interaction is called elastic, based on this process of deformation of the contact layer at the beginning of this stage of interaction. In the case of damaged soil of the contact layer, there are no elastic forces between soil particles (dashed curve 2). In this case, in the interaction process, the soil particles are repacked and the soil structure changes.

In section *AC* of curve 1 (Fig. 1), intensive destruction of the structure of the soil contact layer occurs; this process ends at $u=u_*$, where u_* is the critical value of the relative displacement, at which the structural bonds of the soil contact layer are completely destroyed. In section *CE*, a further increase in the relative displacement does not affect the value of τ , and the Amontons-Coulomb law is fulfilled. It is known that under shear strain of soil, diagram $\tau(\gamma)$ for all soil types with low moisture content (γ is the shear strain of soil) also has the form of curve 1 or 2 (Fig. 1).

The repeated cycle of interaction of the pipeline with soil, when the contact layer is completely damaged, passes along curve 2 (Fig. 1). In section $0 \leq u \leq u_*$, dependence $\tau(u)$ is non-linear in all cases due to changes in the soil structure under the pipeline-soil interaction.

The nonlinearity of the pipeline-soil interaction curves 1, 2 in Fig. 1 is related to the destruction of the structural bonds between the soil particles and their re-packing. On the outer contact surface of the steel pipe and soil (loess, loamy soil), soil particles do not separate from the pipeline [2].

Since in section *CE* of the interaction process, the value of τ depends on σ_N , determined by the Amontons-Coulomb law, then in section *0AC* (curve 1) or *0C* (curve 2) the value of τ should depend on the value of the normal pressure (stress) σ_N acting on the outer surface of the pipeline. Otherwise, there is a discontinuity in the value of τ at point *C*.

As noted above, under the longitudinal interaction of an underground pipeline with the surrounding soil, the soil contact layer of a certain thickness is subjected to shear strain. This soil contact layer on one side is under the shear load of the soil mass, and on the other side is under the pipeline's load. Therefore, the mechanism of shear strain of this layer is rather complicated.

Considering the above, the law of longitudinal interaction of an underground pipeline with soil has the following form [3]:

For $\sigma_N > \sigma_N^*$, $0 \leq u \leq u_*$:

$$\frac{d\tau}{K_{xD}(\sigma_N, I_S)dt} + \mu_S(\sigma_N, I_S, \dot{u}) \frac{\tau}{K_{xS}(\sigma_N, I_S)} = \frac{du}{dt} + \mu_S(\sigma_N, I_S, \dot{u})u \quad (1)$$

For $\sigma_N > \sigma_N^*$, $u > u_*$:

$$\tau = c + f_u \sigma_N \quad (2)$$

For $\sigma_N \leq \sigma_N^*$:

$$\tau = 0, \quad (3)$$

where K_{xD} is the variable dynamic coefficient of soil stiffness (as $\dot{u} \rightarrow \infty$), K_{xS} is the variable static coefficient of soil stiffness (as $\dot{u} \rightarrow 0$), μ_S is the variable parameter of soil shear viscosity,

$\dot{u} = du/dt$ is the velocity of displacement of the pipeline relative to soil, $I_S = u/u_*$ is the parameter characterizing the structural destruction of the soil contact layer, $0 \leq I_S \leq 1$, for $I_S = 0$, the soil contact layer or the contact bonds between the outer surface of the pipeline with soil are not damaged, and for $I_S = 1$, these bonds are completely destroyed, f_u is the internal friction coefficient of soil, σ_N^* is the soil tensile strength (here compressive stresses are assumed positive).

Note that a change in I_S from zero to 1 occurs in each interaction cycle and it is irreversible. In the case of a structurally intact or not completely destroyed soil contact layer, changes in I_S occur along curve 1, and, in the case of a destroyed soil contact layer - along curve 2 (Fig. 1). In both cases, when the underground pipeline interacts with soil, it is considered that there is a change in the structure (destruction, in the case of curve 1 or repacking, in the case of curve 2) of the soil contact layer.

Parameter μ_S and the shear viscosity coefficient η_S are related by:

$$\mu_S = K_{xD} K_{xS} [(K_{xD} - K_{xS}) \eta_S] \quad (4)$$

The functions of stiffness coefficients K_{xD} , K_{xS} are determined from the results of experimental studies conducted by Sultanov [2] and have the following form:

$$K_{xD}(\sigma_N, I_S) = K_{xD}^*(\sigma_N) \exp[\alpha(1 - I_S)] \quad (5)$$

$$K_{xS}(\sigma_N, I_S) = K_{xS}^*(\sigma_N) \exp[\beta(1 - I_S)] \quad (6)$$

where K_{xD}^* and K_{xS}^* are the secant coefficients of dynamic and static stiffness of soil for $u = u_*$, the damaged contact layer of soil.

For an undamaged soil contact layer ($I_S = 0$), from Eqs. (5) and (6) we obtain:

$$K_{xDN} = K_{xD}^* \exp(\alpha), K_{xSN} = K_{xS}^* \exp(\beta) \quad (7)$$

where K_{xDN} and K_{xSN} are the initial values of the stiffness coefficients, α and β are the dimensionless coefficients characterizing the degree of change in K_{xDN} and K_{xSN} .

From Eq. (7), it follows that:

$$\beta = \alpha + \ln(\gamma^* / \gamma_N) \quad (8)$$

where $\gamma^* = K_{xD}^* / K_{xS}^*$, $\gamma_N = K_{xDN} / K_{xSN}$.

It has been already determined that $\gamma^* \geq \gamma_N$ [2], therefore, according to Eq. (8), $\beta \geq \alpha$. Following experimental results obtained by Sultanov [2], the values of β , for curves 1 and 2 (Fig. 1) differ.

Based on the experimental results, the following was obtained [2]:

$$K_{xS}^*(\sigma_N) = K_{NS} \sigma_N; K_{xD}^*(\sigma_N) = K_{ND} \sigma_N \quad (9)$$

where K_{NS} , K_{ND} are static and dynamic interaction coefficients.

Sultanov [2] and Sultanov and Vatin [3] determined that

$$\gamma^* = \gamma_N + (\gamma_N^m - \gamma_N)(\dot{u}/C_S)^\kappa \quad (10)$$

where C_S is the velocity of shear wave propagation in soil.

The value of μ_s under the change in the soil structure is determined from the following equation [3]:

$$\mu_s(\sigma_N, I_s, \dot{u}) = \mu_s^* \exp[\phi(1 - I_s)] \quad (11)$$

where ϕ is the coefficient characterizing the range of change in the parameter of shear viscosity of soil, μ_s^* is the viscosity parameter of the structurally damaged soil.

To determine the approximate values of μ_s^* and η_s^* , the following formulas are obtained, with some assumptions from Eqs. (1) and (4):

$$\mu_s^* = C_s K_{NS} / f; \eta_s^* = \frac{f \sigma_N \gamma_s}{C_s (\gamma_s - 1)} \quad (12)$$

The value of the coefficient of static interaction K_{NS} is determined from the results of experiments by the method given by Sultanov [2] or proposed by Sultanov and Vatin [3], this coefficient and the thickness of the contact layer can be determined through the strength characteristics of soil according to the following relationships:

$$K_{NS} = \frac{f}{\gamma_s u_*} + \frac{c}{\gamma_s \sigma_N u_*} \quad (13)$$

$$\Delta = \frac{\gamma_s G u_*}{f \sigma_N + c} \quad (14)$$

where G is the soil shear modulus.

As can be seen, the interaction model Eq. (1) describing curves 1 and 2 (Fig. 1) is rather complicated. However, an account for the defining factors, such as the velocity of interaction, the destruction of the soil contact layer, the cohesion force, and the force of internal friction of soil, leads to such complex equations. In the simplest cases, without considering these factors, according to Bakhodirov et al. [22], Eq. (1) can be replaced by Eq. (15):

$$\tau = K_x u \quad (15)$$

where K_x for curves 1 and 2 is determined experimentally or from Eqs. (5-6), respectively.

In this case, the law of interaction is determined by Eqs. (15), (2), and (3) considering Eqs. (7-13). As noted by Bakhodirov et al. [22], coefficient K_x is a constant equal to the value of K_{xS} and the interaction curve 2 in Fig. 1, according to Eq. (15), will turn into a straight line, which is not consistent with the experimental results obtained by Sultanov [2].

Experimental studies have established the dependence of the interaction force τ on the depth of the underground pipeline [2]. The static stress (pressure) on the pipe associated with the soil's weight above it, $\sigma_N = \sigma_{NS}$ is normal to the outer surface of the pipeline.

It is known that during the seismic wave propagation, even in cases when the wave front is perpendicular to the axis of the pipeline, there is the dynamic normal stress $\sigma_N = \sigma_{ND}$ acting on the pipe, which is comparable to σ_{NS} , and, sometimes, it can be greater than σ_{NS} . When an arbitrary seismic wave interacts with an underground pipeline, the following formula holds:

$$\sigma_N = \sigma_{NS} + \sigma_{ND} \quad (16)$$

where σ_{NS} is determined by the depth of the pipeline in soil, and σ_{ND} is determined by the pressure of a seismic wave.

When a longitudinal seismic wave propagates parallel to the pipeline's axis, the normal stress σ_{ND} is approximately determined by the following formula:

$$\sigma_{ND} = K_{\sigma} \sigma_g \quad (17)$$

where K_{σ} is the lateral pressure coefficient of soil, and σ_g is the longitudinal seismic stress in soil under longitudinal wave propagation.

In the case of strong earthquakes in loess soils, the approximate maximum value of the longitudinal stress is $\sigma_p^{\max} \leq 0.7$ MPa [3]. Then for $K_{\sigma} = 0.3$, we obtain $\sigma_{ND}^{\max} \leq 0.21$ MPa according to Eq. (17), which conventionally corresponds to a substantially deep embedment of the pipeline ($H \leq 10.5$ m). Therefore, the value of σ_{ND}^{\max} can even exceed σ_{NS} . This shows that calculations conducted according to Eq. (15), for $K_x = \text{const}$, for the seismic stability of underground pipelines, without considering σ_{ND} , are approximate.

Eqs. (1-3) with the corresponding defining relations, Eqs. (4-13), and Eqs. (16, 17) are non-linear interaction laws between an underground pipeline and the surrounding soil.

3. STATEMENT OF THE PROBLEM, BASIC EQUATIONS, AND METHODS FOR THEIR SOLUTION

The embedment of the underground pipeline in soil is shown schematically in Fig. 2a. At a depth of H from the free earth surface there lays a pipeline with an outer diameter D_H and internal diameter D_B , x is the pipeline axis of circular section (Fig. 2a). Due to the cylindrical pipeline, the problem is three-dimensional, which significantly complicates the numerical modeling of the problem under consideration. At the state of rest, the pipeline is subject to static pressure from the overlying soil σ_{NS} . Strictly speaking, the values of σ_{NS} along the perimeter of the outer surface of the pipeline are different, especially for pipes with large external diameters D_H . In the case of seismic wave propagation in soil, for example along the x -axis, additional pressure σ_{ND} is initiated in the pipeline determined by Eq. (17). As a result, the total pressure on the pipeline is $\sigma_N = \sigma_{NS} + \sigma_{ND}$, as was said above. Under the influence of a seismic wave, the soil and the pipeline are strained along the x -axis in different ways and relative displacement is formed in the x -axis direction. This leads to the formation of friction force τ between the pipeline and soil. For F , the longitudinal displacement of soil is u_g and normal dynamic pressure on the pipeline-soil contact surface is σ_{ND} . The values of u_g and σ_{ND} must be determined from the solution to the three-dimensional wave problem. This is a labor-intensive and complex problem. However, this problem can be simplified and reduced to two one-dimensional wave problems: an external one for soil and an internal one - for the pipeline.

These simplifications are as follows:

- the soil, in which the pipeline is embedded is considered an external cylindrical body with external diameter $D_g = 2H + D_H$, internal diameter D_H , and length L , the axis of which coincides with the axis of the pipeline.
 - section $x=0$ is taken as the initial section for the pipeline and soil.
 - longitudinal seismic wave acts in the initial section $x=0$ along the x -axis only in soil.
 - the initial section $x=0$ of the pipeline is load-free and the pipeline is involved in motion under the influence of friction on its outer surface.
 - the underground pipeline and the surrounding soil are considered a coaxial pipe-in-pipe system.

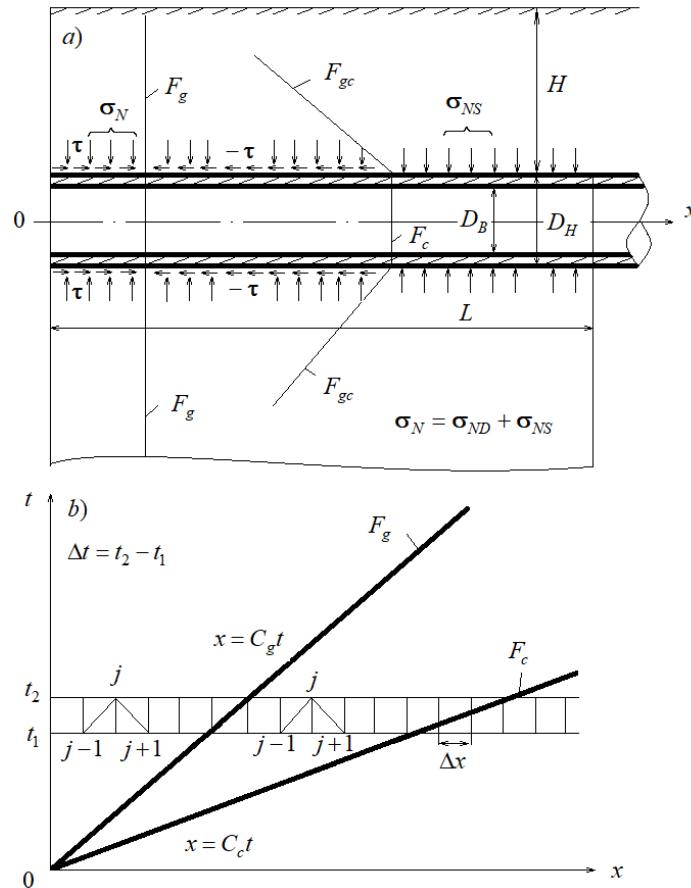


Fig. 2 a) Pipeline location in soil and conditional wave fronts, b) Wave front location on the characteristic plane

The wave pattern for the pipeline and soil on the characteristic plane x, t is shown in Fig. 2b. A plane wave begins to propagate in soil from the initial section $x=0$. The front of this wave F_g remains perpendicular to the x -axis of the pipeline. At section $x=0$ of the pipeline, a frictional force occurs from the soil motion and a plane wave with front F_c begins propagating through the pipeline (Figs. 2a, b). Since the propagation velocities of longitudinal waves in soil and steel pipelines are different, the tilts of these fronts to the x -axis are different. These waves propagate along two characteristic planes x, t . In Fig. 2b, they are combined and shown on the same plane. Numerical calculations are conducted for any time layer t_2 , and in the t_1 layer, the wave parameters are considered known. In this case, the time step dt for both problems is equal, and the space step dx differs. Wave fronts reflected from the pipeline into soil F_{gc} (Figs. 2a, b) and from soil into the pipeline are ignored.

The equations of motion of the pipeline and soil along the x -axis coinciding with the axis of the pipeline, considering the friction force on the surface of their contact, have the following form:

$$\begin{aligned}\rho_{0i}\partial v_i / \partial t - \partial \sigma_i / \partial x + \chi_i \sigma_{\tau i} &= 0 \\ \partial v_i / \partial x - \partial \epsilon_i / \partial t &= 0\end{aligned}\quad (18)$$

where v_i is the particle velocity (mass velocity), σ_i , ϵ_i are longitudinal stresses and strains, ρ_{0i} is the initial density, $\chi_i = \text{sign}(v)$ for the pipeline, $\chi_i = -\text{sign}(v)$ for soil, $v = v_2 = v_g$ is the soil particles velocity, σ_{τ} is the reduced friction force acting per unit length of the pipeline and t denotes the time.

The values of σ_{τ} for the pipeline and soil are determined from the following relation:

$$\sigma_{\tau i} = 4D_{Hi}\tau / (D_{Hi}^2 - D_{Bi}^2) \quad (19)$$

where τ is the friction force (shear stress) determined from Eqs. (1-3), D_{Hi} are the outer diameters of the pipeline and cylinder soil, D_{Bi} are the inner diameters of the pipeline and soil.

The equations of state of the pipeline and soil are assumed linear-viscoelastic (Eyring's model or a model of a standard linear body):

$$\begin{aligned}\frac{d\epsilon_i}{dt} + \mu_i \epsilon_i &= \frac{d\sigma_i}{E_{Di} dt} + \mu \frac{d\sigma_i}{iE_{Si}} \\ \mu_i &= E_{Di} E_{Si} / (E_{Di} - E_{Si}) \eta_i\end{aligned}\quad (20)$$

In Eqs. (18-20), $i = 1, 2$. For $i = 1$, the parameter values refer to the pipeline, and for $i = 2$, to soil. It is known that Eq. (20) for $E_{Si} = E_{Di}$ describes an elastic medium. The parameters introduced in the calculations are $\gamma_c = E_{D1}/E_{S1} = E_{Dc}/E_{Sc}$, $\gamma_g = E_{D2}/E_{S2} = E_{Dg}/E_{Sg}$, where E_{Dc} and E_{Sc} are the dynamic and static strain moduli of pipeline material, respectively, and E_{Dg} and E_{Sg} are the dynamic and static strain moduli of soil. Taking in computer calculations the values of γ_c and γ_g close to 1 or greater than 1, we can examine elastic or viscoelastic pipelines and soils.

The solution to the problem is reduced to integrating the nonlinear system of Eqs. (18) closed by Eq. (20) separately for the pipeline ($i=1$, an inner problem) and soil ($i=2$, an outer problem). These systems are connected by non-linear conditions on the contact surface of the pipeline and soil, which are the laws of change in the interaction force (friction) τ determined by Eqs. (1-3).

Boundary conditions are: for $x=0$, the seismic wave that changes according to the following ratios is set as:

$$\begin{aligned}\sigma &= \sigma_{\max} \sin(\pi t/T), \quad 0 \leq t \leq \theta \\ \sigma &= 0, \quad t > \theta\end{aligned}\quad (21)$$

where T is the half-period of the wave, θ is the wave duration, σ_{\max} is the wave amplitude, σ is the longitudinal stress of the propagating along the x -axis.

The conditions at the wave fronts in soil and the pipeline are zero, and the initial conditions of the problems are zero.

Eqs. (18-20) are hyperbolic, they have characteristic equations and characteristic relations on these equations. By applying the method of characteristics, partial differential Eqs. (18-20) are reduced to ordinary differential equations, solved using the finite difference method in an implicit scheme. Using the described scheme, an algorithm was compiled, and a program for solving the problem in the *FORTTRAN-2005* language implemented on a

computer was developed. Special approaches to the numerical solution of nonlinear systems of equations were developed. Numerical results were obtained as changes in the parameters of waves in soil and the pipeline over time in fixed sections and along the coordinate at fixed time points. The stability of the solution algorithm and the reliability of numerical solutions obtained were substantiated by Sultanov and Vatin [3]. Obtaining numerical solutions for low-frequency waves requires large computer resources. This is due to the discretization steps of the ever-expanding domain of the solution of the wave problem on the characteristic plane x, t . At large discretization steps, the numerical solution instability arises and, at small steps, large resources are required. With the use of powerful modern computers, this problem was overcome and stable numerical solutions to the problem were obtained.

4. RESULTS OBTAINED AND DISCUSSION

A steel pipeline surrounded by soil is considered. Its parameters $\gamma_c = E_{Dc}/E_{Sc}$ and $\gamma_g = E_{Dg}/E_{Sg}$ characterize the stiffness of the pipe material and soil. In numerical calculations, an underground steel pipeline is assumed elastic ($\gamma_c = 1.02$), and the soil is assumed viscoelastic ($\gamma_g = 2$).

In this case, a pipeline surrounded by soil has a length of $L = 1000000$ m so that in the calculation the wave in the pipeline does not reach the final cross-section $x = L$. Then, for greater convenience, the parameters with index c ($i = 1$) refer to the pipeline, and with index g ($i = 2$), they refer to soil.

The following data is used as an initial set for the calculations. Cases obtained under various deviations from this set are discussed separately:

- for underground pipeline:

$$D_{H1} = 0.15 \text{ m}, D_{B1} = 0.14 \text{ m}, \gamma_{gc} = 78 \text{ kN/m}^3, \mu_c = 10^4 \text{ s}^{-1}, C_{0c} = 5000 \text{ m/s}, \gamma_c = 1.02, E_{Dc} = C_{0c}^2 \rho_{0c}, \\ E_{Sc} = E_{Dc} / \gamma_c,$$

- for soil:

$$\gamma_{gg} = 18 \text{ kN/m}^3, C_{0g} = 1000 \text{ m/s}, K_{\sigma} = 0.3, \mu_g = 1000 \text{ s}^{-1}, \\ \gamma_g = 2.0, E_{Dg} = C_{0g}^2 \rho_{0g}, E_{Sg} = E_{Dg} / \gamma_g, D_{H2} = 2.0 \text{ m}, D_{B2} = 0.15 \text{ m},$$

- seismic wave parameters are:

$$T = 1 \text{ s}, \theta = 50 \text{ s}, \sigma_{\max} = 0.35 \text{ MPa},$$

- interaction parameters are:

$$H = 2 \text{ m}, K_N = 100 \text{ m}^{-1}, \beta = 2.5, f_u = 0.5, u_* = 0.003 \text{ m}.$$

The program for the numerical solution to the problem allows us to determine the wave parameters or the variables of the problem separately for soil and the pipeline, and jointly for both cases.

Consider the calculation results. Calculations were conducted for the first arrival (first half-cycle) of the wave only.

Fig. 3 shows changes in the longitudinal stresses in soil.

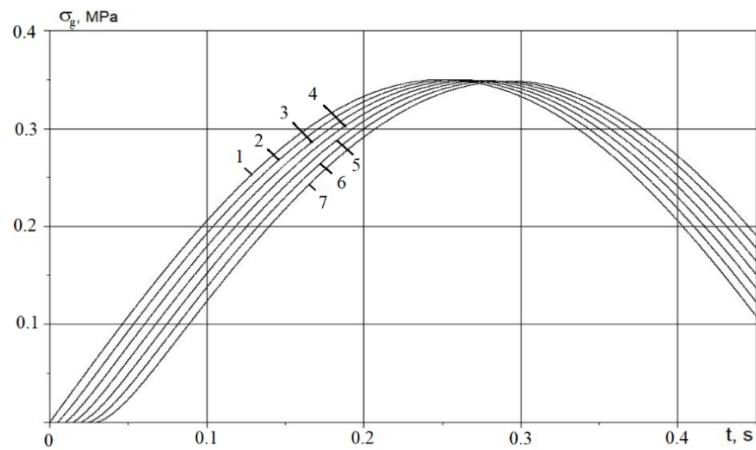


Fig. 3 Longitudinal stresses in soil at distances $x = 0, 5, 10, 15, 20, 25, 30$ m - curves 1-7

Curves 1-7 in Fig. 3 refer to distances $x=0, 5, 10, 15, 20, 25, 30$ m from the initial section $x=0$ of the pipeline and soil. The stress amplitudes in the considered distances are the same $\sigma_{g\max}=0.35$ MPa. The calculation results showed that the wave in soil propagates with this given amplitude and practically does not attenuate. Soil in this case is viscoelastic ($\gamma_g=2.0$).

As seen from Fig. 3, the friction force τ in Eq. (18) does not lead to wave attenuation in soil due to the significant thickness of the soil layer surrounding the underground pipeline ($H=2.0$ m). In all the options of calculations considered below for $\gamma_g=2.0$, the pattern of changes in longitudinal stresses in soil has the form shown in Fig. 3.

Changes in longitudinal stresses in the pipeline in its sections $x=0, 5, 10, 15, 20, 25, 30$ m (curves 1-7) are shown in Fig. 4. The wave (Eq. (21)) does not act in the initial section of the pipeline, this section of the underground pipeline is free from the wave load, and accordingly, the stress is zero (straight line 1, Fig. 4). In subsequent sections of the pipeline, a significant increase in the stress amplitude is observed. In the cross-section at $x=5$ m, the stress amplitude reaches $\sigma_{c\max}=75.7$ MPa (curve 2), at $x=10$ m - 125 MPa (curve 3), at $x=15$ m - 138 MPa (curve 4), at $x=20$ m - 140 MPa (curve 5), at $x=25$ m - 140 MPa (curve 6), and at $x=30$ m - 140 MPa.

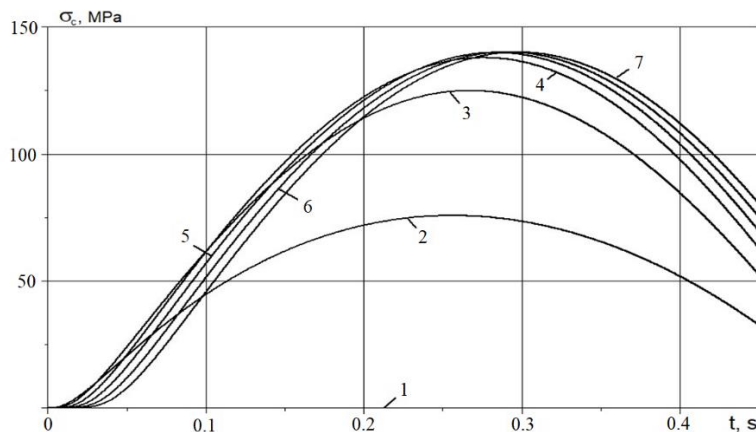


Fig. 4 Longitudinal stresses at $\sigma_{\max}=0.35$ MPa in sections of the underground pipeline $x=0, 5, 10, 15, 20, 25, 30$ m - curves 1-7

The stress amplitude in the pipeline increases with distance from the initial section (curves 1-7, Fig. 4). At distance $x=20$ m, it reaches 140 MPa and remains unchanged. The stress wave propagates with this amplitude through the pipeline without damping. The maximum stress values in the pipeline (140 MPa) are 400 times greater than the stress amplitude in soil - 0.35 MPa. This is due to the active force of the underground pipeline interaction (friction) with soil. This force acting on the outer surface of the underground pipeline, involving the pipeline into motion, increases stresses.

Let us consider the change in the interaction force τ corresponding to this case caused by the relative displacement u (Fig. 5), where curves 1 – 3 refer to distances $x=0, 5,$ and 10 m. In this option of calculations, when the relative displacement reaches the value of $u^*=0.003$ m, the interaction process should occur by the Amontons-Coulomb law.

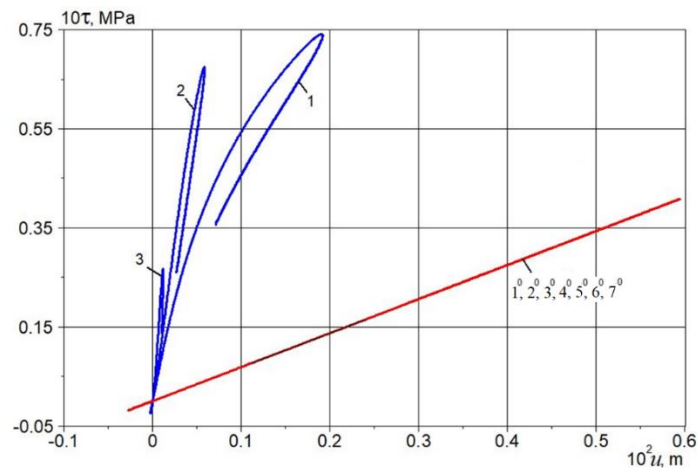


Fig. 5 Changes in the force of interaction (friction) between the underground pipeline and soil at $x=0, 5, 10$ m - curves 1-3

As seen in Fig. 5, the interaction process does not pass to the stage of the Amontons-Coulomb dry friction (curves 1-3). The process of interaction occurs completely according to the law given by Eq. (1). The maximum values of the friction forces significantly decrease with distance and then become negligible (Fig. 6). In Fig. 6, curves 1-4 refer to pipeline sections at $x=15, 20, 25, 30$ m, respectively. As can be seen, the maximum values of the friction force decrease by an order of magnitude compared to the value in the initial sections of the pipeline. This leads to the propagation of a stress wave through the pipeline without attenuation.

Straight lines 1^0-7^0 in Fig. 5 refer to the change in friction force when Eq. (15) is used instead of Eq. (1). In this case, as seen in Fig. 5, the process of interaction occurs in all sections of the pipeline along the same straight line. The values of the friction force are approximately two times less than in the case of Eq. (1). The interaction process passes to the stage of dry friction ($u > u^*=0.003$ m) and is not considered. The significant difference between interaction curves 1-3 in Fig. 5 and curves 1-4 in Fig. 6 from curves 1^0-7^0 in Fig. 5 is the result of considering in Eq. (1) dynamic pressure normal to the outer surface of the pipeline, structural changes in the contact layer of soil, and interaction rates. These parameters are not considered

in the case of the law given by Eq. (15) (curves 1⁰-7⁰). An account for these parameters leads to a completely different pattern of the interaction process between the pipeline and soil. In this case, the law of interaction becomes essentially non-linear.

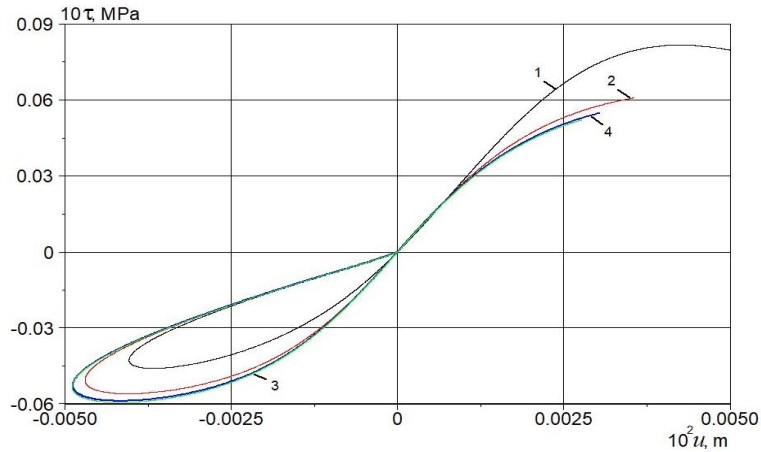


Fig. 6 Changes in the force of interaction (friction) between the underground pipeline and soil at $x=15, 20, 25, 30$ m - curves 1-4

An increase in the amplitude of the propagating wave in section $x=0$ to $\sigma_{\max} = 0.5$ MPa, leads to a greater increase in the stress amplitude in the sections of the pipeline (Fig. 7).

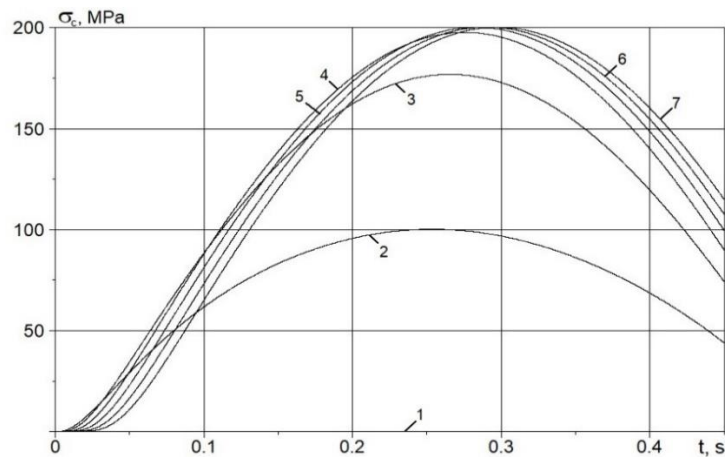


Fig. 7 Longitudinal stresses at $\sigma_{\max}=0.5$ MPa in sections of the underground pipeline $x=0, 5, 10, 15, 20, 25, 30$ m - curves 1-7

In this option, the steady-state stress amplitude reaches $\sigma_{c\max} = 200$ MPa (curves 1-7, Fig. 7). Curves 1-7 in Fig. 7 refer to the same sections of the pipeline as curves 1-7 in Fig. 4. However, the stress amplitude in the pipeline in this option is 400 times greater than the

amplitude of the wave in soil ($\sigma_{\max} = 0.5$ MPa). The changes in the interaction force corresponding to this case are shown in Fig. 8.

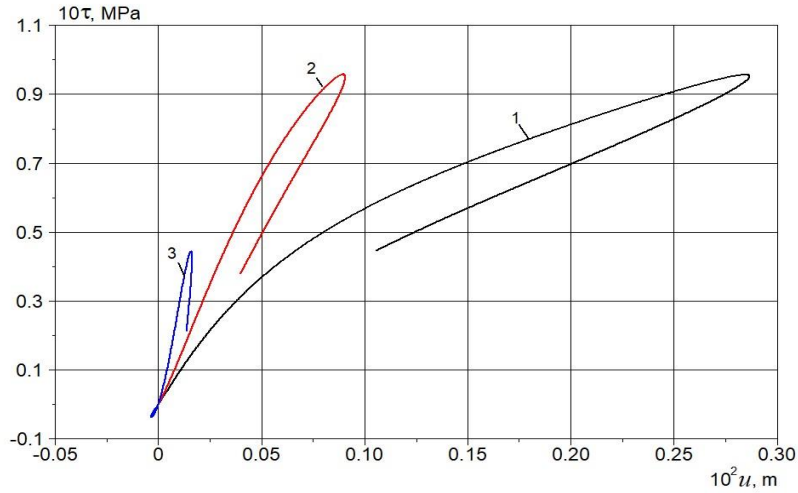


Fig. 8 Changes in the interaction force in sections of the underground pipeline at $x=0, 5, 10$ m - curves 1-3

An increase in the wave amplitude in soil also leads to an increase in the value of the friction forces in the outer surface of the underground pipeline. Compared to the previous case, the value of τ increases by 1.3 times at the initial section of the pipeline. However, the process of interaction in this case does not pass to the stage of dry friction. The maximum value of τ , at the distance from the initial section of the pipeline $x=10$ m (curve 3, Fig. 8), is approximately two times less compared to the initial section $x=0$ (curve 1, Fig. 7). As the calculation results show, at a distance of $x=30$ m, the values of $\tau=0.08$ MPa are 11 times less than in the initial section. A decrease in the value of τ with distance allows for the longitudinal waves initiated in the initial section (up to 15-20 m) of the pipeline, to propagate in the pipeline without attenuation.

An increase in the maximum value of the wave stress in the initial section up to $\sigma_{\max}=0.7$ MPa, which corresponds to destructive earthquakes, results in the stress increase in the pipeline to $\sigma_{\text{cmax}} = 280$ MPa, the value of τ increases to 0.13 MPa. In this case, the pipeline experiences plastic strain under such stresses, which contradicts the initial assumption that the pipeline is elastic. In cases where the longitudinal stress in the pipeline exceeds the elastic limit of the material, we will assume that the pipeline is damaged. More reliable results can be obtained when considering the elastic-plastic properties of the pipeline material, which is a task for future studies.

In this case, the interaction process passes to the stage of the Amontons-Coulomb dry friction only in the initial section of the pipeline up to $x = 5$ m. Beyond this distance, the interaction process occurs according to Eq. (1).

In the case of initial data $\sigma_{\max} = 0.35$ MPa, like the case shown in Fig. 4, the values are $K_{\sigma} = 0.1$, $K_N = 500 \text{ m}^{-1}$ and $f_u = 0.3$, other parameters remain unchanged. The patterns of interaction are shown in Fig. 9.

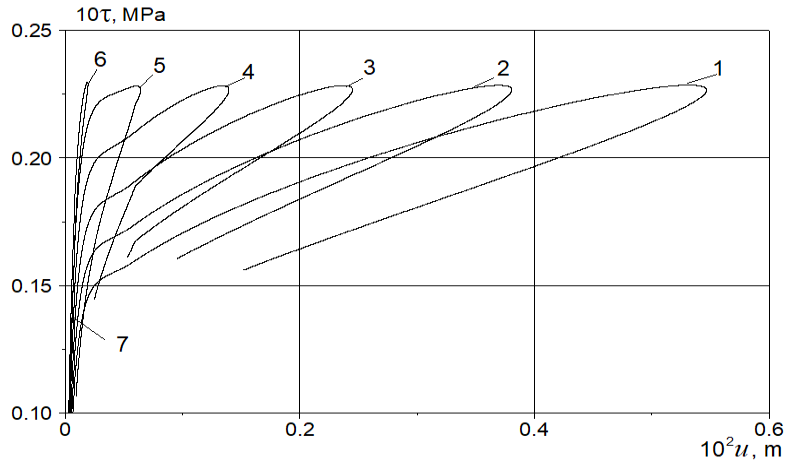


Fig. 9 Changes in the interaction force in sections of the underground pipeline at $x=0, 5, 10, 15, 20, 25, 30$ m - curves 1-7

In this case, when the values are $u^* = 0.0006$ m, and in the initial section of the pipeline up to $x=15$ m, the interaction process occurs mainly in the second stage – the Amontons-Coulomb stage (curves 1-4). At distance $x=20$ m, the process of interaction partially occurs by the law of dry friction (Eq. (2)). In the section of the pipeline $x = 20$ m (curve 5), the relative displacement reaches the value of $u = 0.65 \cdot 10^{-3}$ m, which slightly exceeds the values of u^* . Farther along the contact surface of the pipeline, the law of interaction Eq. (1) is fulfilled. Despite the same wave amplitude values in soil $\sigma_{\max} = 0.35$ MPa, as in Fig. 4, the maximum value of the friction force τ is 0.023 MPa at $x=0$, which is approximately three times less than in Fig. 5. Here, the value of the stress amplitude is $\sigma_{c\max} = 130$ MPa and it is only 7% less than in Fig. 4. These results show that the longitudinal stresses in the pipeline under seismic impacts mainly depend on the longitudinal seismic stresses in soil, and, therefore, on the seismic pressure on the pipeline.

Thus, in the contact interaction of an underground pipeline with soil under seismic effects, the laws of interaction (Eqs. (1-3)) adequately describe the interaction process. The numerical results obtained above show that when determining the stresses in the pipeline, the correct choice of the law of interaction between the pipeline and soil is of paramount importance.

Sultanov and Vatin [3] showed that under strong ground motion, longitudinal stresses in underground pipelines may reach up to $\sigma_{c\max} = 85$ MPa and more. The results obtained confirm this statement.

5. CONCLUSIONS

The proposed two-stage nonlinear law of interaction of an underground pipeline with the surrounding soil describes the interaction process and is applicable in calculations to determine longitudinal seismic stresses in the pipeline.

The law of interaction considered in the study, in contrast to the laws used nowadays when solving problems of the underground pipeline strength under seismic impacts, accounts for the transition of the process of the pipeline-soil interaction to the stage of Amontons-Coulomb friction and the dependence of the friction forces caused by the wave pressure in soil on the pipeline during both stages. This law also considers the destruction of the soil contact layer around the pipeline when it interacts with soil and the rate of interaction.

The numerical solution to the wave problems considered for the pipeline-soil system showed that seismic stresses in the pipeline increase manifold compared to the longitudinal stresses in soil. This is explained by the lower stiffness of the soil surrounding the pipeline compared to the steel pipeline rigidity and the nonlinear properties of the interaction law. In this case, the dynamic soil pressure on the pipeline is determinant. As a result of the greater deformability of soil, the interaction force (friction) is active and leads to a significant increase in stresses in the pipeline.

Interaction force (friction), actively acting in the initial section of the pipeline, creates a powerful wave with an amplitude many times greater than the wave in soil. Farther the value of the friction force between the pipeline and soil decreases, and this wave propagates through the pipeline with insignificant attenuation (for a low-frequency excitation wave and viscoelastic soil).

As the calculation results showed, longitudinal stress waves and their amplitudes in underground pipelines strongly depend on the law describing the process of interaction of the underground pipeline with soil. This article discusses a more realistic soil-pipeline interaction law.

Acknowledgement: *The research was conducted at the expense of basic budget funding from the Academy of Sciences of the Republic of Uzbekistan.*

REFERENCES

1. Popov, V.L., Heß, M., 2015, *Method of Dimensionality Reduction in Contact Mechanics and Friction*, Edition: 1st Publisher: Springer, 253 p.
2. Sultanov, K.S., 1993, *Laws governing the interaction of underground structures with soil during their relative displacement*, International Applied Mechanics, 29(3), pp. 217–223.
3. Sultanov, K.S., Vatin, N.I., 2021, *Wave Theory of Seismic Resistance of Underground Pipelines*, Applied Sciences, 11(4), 1797.
4. Kwong, N.S., Jaiswal, K.S., 2023, *A Methodology to Combine Shaking and Ground Failure Models for Forecasting Seismic Damage to Buried Pipeline Networks*, Bulletin of the Seismological Society of America, 113(6), pp. 2574–2595.
5. Musa, A.B., 2013, *Numerical solution of wave propagation in viscoelastic rods (standard linear solid model)*, IOP Conference Series: Earth and Environmental Science, 16, 012039.
6. Fan, K. Liu, J. Wang, J. Jin, C., 2023, *Evolution Analysis of Strain Waves for the Fractal Nonlinear Propagation Equation of Longitudinal Waves in a Rod*, Fractal and Fractional, 7(8), 586.
7. Popov, V.L., 2017, *Contact Mechanics and friction. Physical principles and applications*, 2nd Edition, Springer.
8. Zhang, R., Wang, C., Li, S., Zhang, J., Liu, W., 2023, *Numerical Simulation Study on the Performance of Buried Pipelines under the Action of Faults*, Applied Sciences, 13(20), 11266.

9. Xue, J., Ji, L., 2024, *Mechanical Properties of Buried Steel Pipe With Polyurethane Isolation Layer Under Strike-Slip Fault*, Journal of Pressure Vessel Technology, Transactions of the ASME, 146(1), 011901.
10. Yiğit, A., Lav, M.A., Gedikli, A., 2018, *Vulnerability of Natural Gas Pipelines under Earthquake Effects*, Journal of Pipeline Systems Engineering and Practice, 9(1), 04017036
11. Demirci, H.E., Karaman, M., Bhattacharya, S., 2021, *Behaviour of buried continuous pipelines crossing strike-slip faults: Experimental and numerical study*, Journal of Natural Gas Science and Engineering, 92, 103980.
12. Yang, C., Li, S., 2021, *Theoretical analysis and finite element simulation of pipeline structure in liquefied soil*, Heliyon, 7(7), e07480.
13. Boorboor, A., Hosseini, M., 2015, *Evaluation of Water Distribution Jointed Pipe Networks under Transient Ground Motions*, Open Journal Civil Engineering, 5(2), pp. 190–202.
14. Boorboor, A., Hosseini, M., 2015, *Sensitivity Analysis of Buried Jointed Pipelines Subjected to Earthquake Waves*, Open Journal Earthquake Research, 4(2), pp. 74–84.
15. Izadi, M., Bargi, K., 2019, *Improvement of mechanical behavior of buried pipelines subjected to strike-slip faulting using textured pipeline*. Frontiers of Structural and Civil Engineering, 13(5), pp. 1105–1119.
16. Vazouras, P., Dakoulas, P., Karamanos, S.A., 2015, *Pipe-soil interaction and pipeline performance under strike-slip fault movements*, Soil Dynamics and Earthquake Engineering, 72, pp. 48–65.
17. Valsamis, A.I., Bouckovalas, G.D., 2020, *Analytical methodology for the verification of buried steel pipelines with flexible joints crossing strike-slip faults*, Soil Dynamics and Earthquake Engineering, 138, 106280.
18. Dai, J., Wang, L., Hu, C., Zhang, G., 2021, *Experimental Study on Seismic Response of Buried Oil and Gas Pipeline Soil Layers under Lateral Multipoint Excitation*, Shock and Vibration, 2021, 9887140.
19. Huang, D., Tang, A., Wang, Z., 2020, *Analysis of pipe-soil interactions using Goodman contact element under seismic action*, Soil Dynamics and Earthquake Engineering, 139, 106290.
20. Sarvanis, G.C., Karamanos, S.A., Vazouras, P., Mecozzi, E., Lucci, A., Dakoulas, P., 2018, *Permanent earthquake-induced actions in buried pipelines: Numerical modeling and experimental verification*, Earthquake Engineering and Structural Dynamics, 47(4), pp. 966–987.
21. Psyrras, N.K., Sextos, A.G., 2018, *Safety of buried steel natural gas pipelines under earthquake-induced ground shaking: A review*, Soil Dynamics and Earthquake Engineering, 106, pp. 254–277.
22. Bakhodirov, A.A., Ismailova, S.I., Sultanov, K.S., 2015, *Dynamic deformation of the contact layer when there is shear interaction between a body and the soil*, Journal of Applied Mathematics and Mechanics, 79(6), pp. 587–595.
23. Amabili, M., 2019, *Derivation of nonlinear damping from viscoelasticity in case of nonlinear vibrations*, Nonlinear Dynamics, 97(3), pp. 1785–1797.
24. Sultanov, K.S., Khusanov, B.E., Rikhsieva, B.B., 2020, *Longitudinal waves in a cylinder with active external friction in a limited area*, Journal of Physics: Conference Series, 1546(1), 012140.
25. Jiao, W., Xu, J., Tian, J., Xie, X., Du, G., 2021, *Seismic response analysis of buried pipelines with the high drop*, International Journal of Pressure Vessels and Piping, 191, 104379.
26. Yan, K., Zhang, J., Wang, Z., Liao, W., Wu, Z., 2018, *Seismic responses of deep buried pipeline under non-uniform excitations from large scale shaking table test*, Soil Dynamics and Earthquake Engineering, 113, pp. 180–192.
27. Guo, Z., Han, J., Hesham, E., Naggar, M., Hou, B., Zhong, Z., Du, X., 2023, *Numerical analysis of buried pipelines response to bidirectional non-uniform seismic excitation*, Computers and Geotechnics, 159, 105485.